Pseudo-Weak-Phase-Object Approximation in High-Resolution Electron Microscopy. II. Feasibility of Directly Observing Li+ *

By D. Tang, C. M. Teng, J. Zou† and F. H. Li

Institute of Physics, Academia Sinica, Beijing, China

Abstract

Images of $Li_2Ti_3O_7$ were calculated with the multislice method and observed with a JEM-200CX electron microscope. Both calculated and observed images show that Li^+ ions can be seen intuitively under an optimum imaging condition as is predicted by the theory of the pseudo-weak-phase-object approximation.

1. Introduction

In the earlier papers in this study (Li & Tang, 1984, 1985) the dependence of image contrast on crystal thickness was discussed. When the crystal is too thick to allow the weak-phase-object approximation (WPOA) to hold, it was shown that with increasing crystal thickness the image contrast of light atoms increases more rapidly than that of heavy atoms. Hence, crystals too thick for weak-phase-object approximation to hold but thinner than the critical thickness have been treated as pseudo-weak phase objects. Under the optimum imaging condition the image intensity can be expressed as

$$I(r) = 1 - 2\sigma\varphi'(r). \qquad (1)$$

Here $\varphi'(r)$ is the modified projected potential distribution function (PPDF) which can be treated as the PPDF of an imaginary isomorph of the examined crystal where real atoms are replaced by imaginary ones. The constituent heavy and light atoms of the imaginary isomorph are respectively lighter and heavier than those of the real crystal. This indicates the possibility of preferentially revealing different kinds of atoms by choosing observation regions of different thicknesses in the crystal examined.

It was found by the HREM (high-resolution electron microscopy) observation on the mineral cebaite $Ba_3Ce_2(CO_3)_5F_2$ that within a certain range of crystal thicknesses the image contrast is sensitive to the positions of light atoms (C, O, F) and hence the positions of these light atoms were determined by HREM (Li
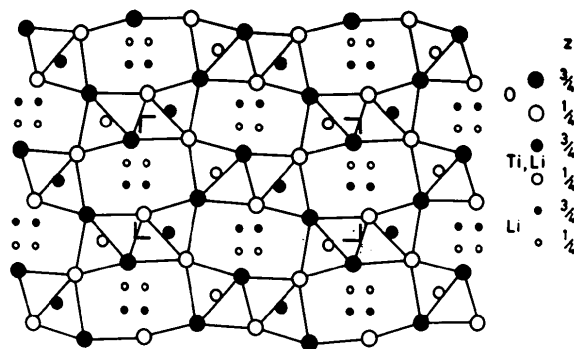

Fig. 1. Structure model of $Li_2Ti_3O_7$ projected along [001]. Li ions are in the large channels.
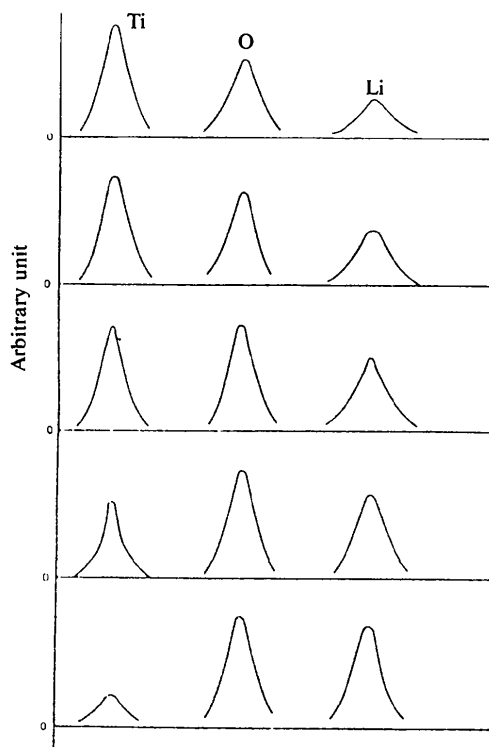

Fig. 2. Schematic diagram showing the relative variation of the image contrast for atoms of Ti, O and Li with crystal thickness. The increase of crystal thickness, successively from top to bottom in the diagram, leads to an enhancement of the image contrast of the light atom Li.

& Hashimoto, 1984). The purpose of this work is to explore whether atoms as light as lithium can be seen intuitively in the image.

IMAGES OF $Li_2Ti_3O_7$
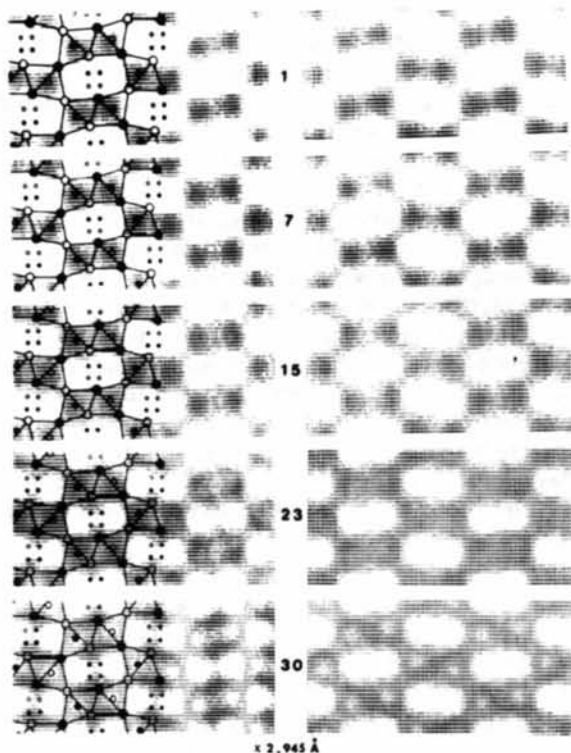

Fig. 3. Calculated images of $Li_2Ti_3O_7$ (left column) and of a model similar to $Li_2Ti_3O_7$ but with large channels empty (right column) for accelerating voltage 200 kV and underfocus 600 Å. The slice number is shown between the two columns and the slice thickness is given at the bottom.
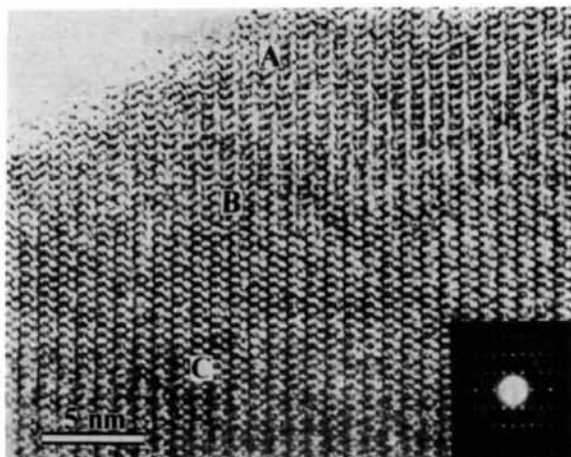

Fig. 4. High-resolution electron microscopic image of a wedge-shaped crystal of $Li_2Ti_3O_7$. Radius of the objective aperture is 0·63 Å^{-1}. Regions A, B and C are shown enlarged in Fig. 5. (1 nm $\equiv$ 10 Å.)

2. Projected structure model and calculated images of $Li_2Ti_3O_7$

A crystal of $Li_2Ti_3O_7$ was used as the sample. The projected structure model along [001] is shown in Fig. 1 (Morosin & Mikkelsen, 1979; Mikkelsen, 1979).
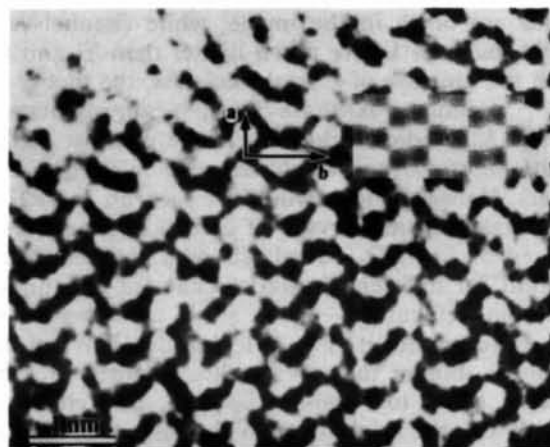
(a)
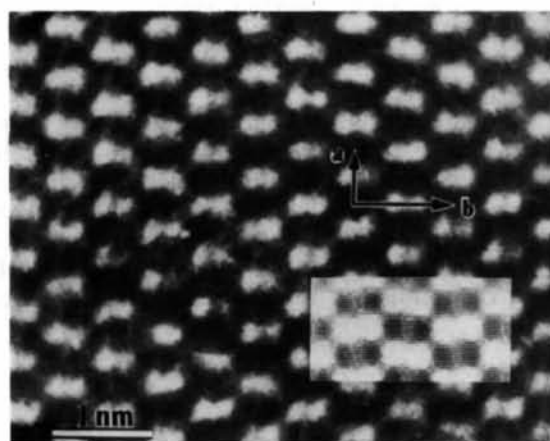
(b)
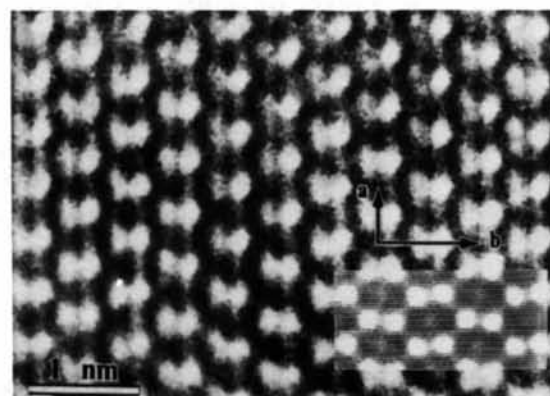
(c)

Fig. 5. Enlarged images of regions A, B and C of Fig. 4. Inserted simulated images of $Li_2Ti_3O_7$ are calculated for crystal thickness about (a) 21 Å, (b) 44 Å and (c) 68 Å. Li ions are not seen in (a), the large channels begin to contract in (b), and Li ions give strong image contrast in (c).

The large channels are occupied by Li ions. Fig. 2 is a schematic diagram of the relative image contrast variation with crystal thickness, which increases successively from top to bottom, for atoms of Ti, O and Li. When the crystal is very thin, *i.e.* the WPOA (weak-phase-object approximation) can hold, Ti atoms are black in the image, while channels are bright, because Li are much lighter than Ti and O. With the increase of crystal thickness, the theory of the pseudo-weak-phase-object approximation (PWPOA) predicted that the image contrast at the positions of Li ions would increase relative to the others. Hence, Li ions would be seen on a HREM image taken from a crystal of correct thickness. The images of $Li_2Ti_3O_7$ calculated with the multislice method for different crystal thicknesses and under optimum defocus of -600 Å are in agreement with the above argument (Fig. 3, left column). When the crystal is thinner than 44 Å (slice number 15), the contrast of Li ions cannot be seen, and channels appear as large bright dots. With increase of crystal thickness the contrast of Li ions increases relatively, so that the contrast of channels begins to contract in the centre. When the crystal thickness reaches 68 Å (slice number 23) each large bright dot splits into two small bright dots.

As we know, the image contrast of an empty channel will change with change of crystal thickness. In order to confirm that the contrast variation at channel positions shown in the left column of Fig. 3 indeed comes from Li ions, images have been calculated for a model similar to $Li_2Ti_3O_7$ but with empty channels (Fig. 3, right column). It can be seen that the large

bright dots do not split although the channel contrast also contracts with increase in crystal thickness.

3. Observed images of $Li_2Ti_3O_7$

An $Li_2Ti_3O_7$ crystal was grown by the Czochralski method (Jiang, Zhang, Shu & Sheng, 1985). The powder samples were observed with a JEOL-200CX high-resolution electron microscope equipped with a top-entry stage. Fig. 4 shows an image taken from a wedge-shaped crystal under an accelerating voltage of 200 kV. Figs. 5(*a*), 5(*b*) and 5(*c*) are enlarged images corresponding to regions *A*, *B* and *C* in Fig. 4, respectively. It can be seen that the inserted calculated images, for crystal thicknesses 21, 44 and 68 Å and underfocus 600 Å, are in good agreement with the observed ones. In Fig. 5(*a*) Li ions have no contrast at all and channels appear as large bright dots. In Fig. 5(*b*) the channels begin to contract in their centres. In Fig. 5(*c*) the channels split into two separate bright dots. This indicates that the observed image contrast at the positions of the Li ions increases with the increase of crystal thickness more rapidly than for heavier atoms.

References

JIANG, Y. D., ZHANG, Y. Z., SHU, Q. M. & SHENG, X. (1985). *J. Chin. Silic. Soc.* **13**(1), 92–96.
LI, F. H. & HASHIMOTO, H. (1984). *Acta Cryst.* **B40**, 454–461.
LI, F. H. & TANG, D. (1984). *Acta Phys. Sin.* **33**, 1196–1197.
LI, F. H. & TANG, D. (1985). *Acta Cryst.* **A41**, 376–382.
MIKKELSEN, J. C. (1979). *J. Cryst. Growth*, **47**, 659–665.
MOROSIN, B. & MIKKELSEN, J. C. (1979). *Acta Cryst.* **B35**, 798–800.

Un Nouvel Exemple de Structures-Vernier: Les Phases $Zr_m(F,O)_{2m+1}$ de Type Fluorine Excédentaire en Anions

PAR R. PAPIERNIK ET B. FRIT*

Laboratoire de Chimie Minérale Structurale, UA CNRS n° 320, UER des Sciences, 123 avenue A. Thomas, 87060 Limoges CEDEX, France

Abstract

By solid-state reaction under high pressure (8 GPa) from 1273 up to 1473 K between ZrO_2 and ZrF_4 compounds, an apparently continuous sequence of ordered orthorhombic structures has been synthe-

sized in the composition range $2\cdot105 \le x \le 2\cdot205$ of $Zr(F, O)_{2+x}$. It may be approximated to more or less regular intergrowths of a limited number of members of a homologous series $Zr_m(F,O)_{2m+1}$ with a few integral *m* values $(5 \le m \le 9)$. The anions in excess of those in the fluorite type are accommodated by a one-dimensional vernier process, half of the 4^4 anion layers being periodically changed into compacted 3^6

_____

* Auteur auquel toute correspondance devra être adressée.